



# Soil erosion and radiocesium migration during the snowmelt period in grasslands and forested areas of Miyagi prefecture, Japan

Mikhail Komissarov · Shin-ichiro Ogura

Received: 5 April 2020 / Accepted: 5 August 2020 / Published online: 13 August 2020  
© Springer Nature Switzerland AG 2020

**Abstract** This study aimed to examine the influence of snowmelt on soil erosion processes in mountainous landscapes in the Miyagi prefecture of Japan. The investigated slopes had different expositions and were covered with grasslands and forests. The snowpack thickness, soil frost depth, volume of surface runoff, physicochemical properties of the soil and sediments, cesium composition of the snow and meltwater, and air dose rate were determined. In mid-February, snow cover reached its maximum thickness (100–179 cm). In the forest, the snow depth was always lower by 15–20 cm. The soil did not freeze in winter in any of the plots. Surface runoff was observed only in the grassland plots and depended on the slope aspect. The total volume of surface runoff ranged from 31 to 52 mm and snowmelt soil losses ranged from 2 to 9 kg ha<sup>-1</sup> DM. Radiocesium concentrations in runoff samples ranged from 0.1 to 8.4 Bq L<sup>-1</sup>, below the standard limit for drinking water in Japan (10 Bq L<sup>-1</sup>). The average organic matter content of the sampled sediments was 0.4%, higher than that in the surface soil. The silt fraction in sediments became dominant for particle size distribution, and the activity concentration of total radiocesium was, on

average, 250 Bq kg<sup>-1</sup>. The air dose rate was always lower than the maximum permissible level (0.2 μSv h<sup>-1</sup>) and varied from 0.02 to 0.09 μSv h<sup>-1</sup> in winter, and from 0.08 to 0.13 μSv h<sup>-1</sup> at times of the year without snow.

**Keywords** Air dose rate · Cesium · Sediment · Snowmelt · Water erosion

## Introduction

Erosion is a global environmental problem and the prevailing cause of soil degradation. This causes immense economic and environmental damage because soil is the key means of agricultural production and an essential component of the biosphere (Uri 2001; Rumpel et al. 2006). The total loss of global productive land due to erosion is estimated at approximately 6.7 million ha, and the annual loss from the productive layer is estimated at 24 million t (Lal 1991). The economic cost of the loss of agricultural land by soil erosion is estimated to be approximately US\$400 billion per year (IAEA 2011), which is comparable to the gross domestic product of an average European country. Uri (2001) estimates that soil erosion in the USA costs the nation approximately \$37.6 billion each year in loss of productivity.

Water erosion can be caused by rainfall, irrigation, and snowmelt. Spring snowmelt runoff commonly causes water erosion in areas where freezing temperatures and snow cover persist for months (Demidov et al. 1995; Ollesch et al. 2005). The intensity of this erosion

---

M. Komissarov (✉)  
Ufa Institute of Biology UFRS, Russian Academy of Sciences, Pr.  
Oktyabrya 69, Ufa 450054, Russia  
e-mail: mkomissarov@list.ru

S.-i. Ogura  
Graduate School of Agricultural Science, Tohoku University,  
232-3 Yomogita, Naruko-onsen, Osaki 989-6711, Japan

depends on a variety of factors, of which the most important are the amount of snowpack, the slope gradient, the land use type, and the frost penetration depth (Lindström et al. 2002; Tanasienko et al. 2009). Dube and Mailloux (1969) and Kirby and Mehuis (1987) have thus reported that snowmelt runoff could explain from 40 to 88% of annual erosion. Erosion caused by snowmelt runoff washes off soil, and with it nutrients, fertilizers, herbicides, pesticides, and pollutants (e.g., radioisotopes), into lakes, ponds, rivers, and reservoirs (Muthanna et al. 2007; Grismer 2013). Thus, hydrological systems and their associated habitats are subjected to increased stress through the input of numerous contaminants. This is of considerable concern and means that erosion leads to a deterioration in water quality, resulting from siltation and eutrophication (Sayer and Neil 2001), and an increase in fish mortality.

Japan receives some of the heaviest snowfall in the world, with an annual average snow depth of over 1.0 m in mountain areas and in the western areas of Japan, adjacent to the Japan Sea (Matsuura et al. 2017). Snowfall and snowmelt play important roles in maintaining the water resources of Japan (Kazama and Sawamoto 1995). Snowmelt provides irrigation for paddy fields in spring, but heavy snowfall can result in severe damage to infrastructure. Heavy snowfall also creates hazards for humans through the destruction of buildings and electricity lines and disruption to transport systems (Kawagoe et al. 2009).

In Japan, some efforts have been made to estimate contemporary rates of erosion using the sediment delivery ratio to the reservoirs (Yoshikawa 1974; Ashida and Kira 1975), whereby the mean rates of erosion in the mountainous regions of Japan seem to be in the order of  $500 \text{ m}^3 \text{ km}^{-2} \text{ year}^{-1}$ , 10 times the world average. Rates are particularly high in the Central Highland and Outer Zone of SW Japan, where downpours commonly fracture Quaternary uplift (1000–1500 m), and average sediment yield is 1000–5000  $\text{m}^3 \text{ km}^{-2} \text{ year}^{-1}$ . According to Yoshikawa (1974), the highest rate ( $\sim 10,000 \text{ m}^3 \text{ km}^{-2} \text{ year}^{-1}$ ) was observed in reservoir sediments at Kurobe IV dam, in the uppermost Kurobe River area characterized by subalpine and alpine habitats which rise up to the North Japan Alps (2500–3000 m a.s.l.). In contrast, erosion rates in the hilly regions are relatively low, e.g., in the central parts of the Abukuma and Chugoku Mountains, characterized by undulating landscapes, rates of erosion may be 10–50  $\text{m}^3 \text{ km}^{-2} \text{ year}^{-1}$ . Although data are scarce, measurements at some experimental watersheds have shown that the rates of sediment yield from hills and uplands, which are covered

with thick, well-managed forests, are generally from 10 to  $50 \text{ m}^3 \text{ km}^{-2} \text{ year}^{-1}$  or less. These values can be considered as background erosion rates in the hills and uplands where urbanization and agricultural development are ongoing, causing modifications to the natural landscape (Kadomura 1980).

It is well known that the damage to the Fukushima Daiichi Nuclear Power Plant (NPP) incurred in the Great East Japan Earthquake and tsunami on March 11, 2011 resulted in serious radioactive pollution over Eastern Japan. In Miyagi prefecture, the radioactive contamination of ecosystems by radiocesium (r-Cs;  $^{134}\text{Cs}$  and  $^{137}\text{Cs}$ ) is also high (Ogura et al. 2014; Komissarov et al. 2017), and in July 2014 was  $16 \text{ kBq m}^{-2}$  (Komissarov and Ogura 2017). Before the Fukushima-1 accident, the soil contamination density of  $^{137}\text{Cs}$  in the study region was nine times lower compared with that in 2014 and amounted to  $1.7 \pm 1.4 \text{ kBq m}^{-2}$  (Miura et al. 2015).

Information about soil erosion rates in Miyagi prefecture is still minimal, especially that about snowmelt soil losses. During erosion processes when polluted sediments are transported from mountainous areas, they could contaminate the agricultural foothills (and crops) and also add impurities to the drinking water in ponds and rivers. Thus, data about soil erosion rates is highly necessary and relevant.

The main aim of the present study is to answer the following question:

Does snowmelt lead to runoff, soil erosion, and r-Cs migration in the subalpine areas of Miyagi prefecture?

The specific topics of this study were to investigate:

1. Snowmelt runoff parameters in grasslands and forest landscapes in terms of exposure
2. The removal of r-Cs from soil and its dissolved activity concentration in snowmelt runoff
3. The features in physicochemical properties and particle size distribution of the sediments
4. The changing of air dose rate depending on catchment type (grassland/forest) and season (winter/summer)

## Material and methods

### Site description

The study was conducted in a mountainous area (Kitayama,  $38^\circ 46' \text{ N}$ ,  $140^\circ 44' \text{ E}$ ) near the Kawatabi

Field Scientific Centre of Tohoku University, 60 km north of Sendai and 150 km north-west of Fukushima Daiichi NPP Japan (Fig. 1). The climate in this region is temperate, with a mean annual temperature of 10.2 °C and a mean annual precipitation of 1660 mm based on records for the period 1979–2000. Most of the forest areas were previously utilized as fuel wood coppices or hay meadows, but some were abandoned in the 1950s and have regenerated naturally as secondary deciduous forests.

It should be noted that 70% of the Japanese archipelago is mountainous. Approximately 25 million hectares, corresponding to two-thirds (Kato et al. 2012) of Japan's national land area, is covered by forests, most of which are in steep mountainous areas. The remainder of the mountain slopes is usually covered by grassland (pastures).

The landscape of the study site is characterized by semi-natural pastures surrounded by secondary forests on a moderate slope. The soils are derived from acidic volcanic ash and are classified as haplic, non-allophanic andosols according to the Soil Classification for Cultivated Soils in Japan (Classification Committee of Cultivated Soils 1996), or as Alic Hapludands according to the Soil Taxonomy of the Soil Survey Staff (1999). The semi-natural pasture has not received fertilizer or other treatments recently, and there are no exotic species present (Yoshihara and Sato 2013).

Grassland and forest landscapes on mountain slopes with different geographical characteristics were investigated. The four investigated experimental catchments were situated at the main aspects of the slopes at altitudes from 580 to 620 m a.s.l. and with angles of 11–20 degrees. Each catchment consisted of two plots: one grassland and one forest site (Fig. 1; Table 1). The length, angle, and exposition of the slopes were determined with a tape-line, alidade, and compass, and a Global Positioning System was used for exact recording of coordinates.

#### Field and laboratory measurements

For soil type characterization and soil sampling, a 1-m-wide and 3-m-long three profile pits were dug in each plot along the slope: one at the top of the slope, one in the middle (intermediate location), and one at the bottom of the slope. Soil was sampled from different levels (0–2.5 cm, 2.5–5 cm, then at 10-cm intervals until the parent material layer) from all 24 profile pits (four

catchments areas, each with two plots, at three different positions on the slope). The stones and tree/plant roots were removed from the soil and sediments, which was then dried in an oven at 105 °C and then ground in a mortar and manually sieved through a 2-mm sieve. The organic matter content was determined by measuring loss during ignition in a muffle furnace at 450 °C for 8 h. The physicochemical properties of the samples were determined for the < 2 mm fraction of the soil samples. The particle size distribution (sand > 50 µm, silt 2–50 µm, and clay < 2 µm) in each sample was analyzed using a laser diffraction particle size analyzer (SALD-3100, Shimadzu Co., Ltd., Kyoto, Japan). The bulk density was determined from the dry weight and volume of the undisturbed soil and sediment samples.

The  $^{134}\text{Cs}$  and  $^{137}\text{Cs}$  activity concentration in the soil, sediments, and in the snow and runoff water was determined by gamma ( $\gamma$ ) spectrometry using HPGe detectors (PerkinElmer WIZARD<sup>2</sup> 2480, Waltham, MA, USA). Measuring times (usually 30 min per sample) was chosen in order to achieve a statistical uncertainty less than 5%. The r-Cs concentration was expressed as the concentration of  $^{134}\text{Cs}$  and  $^{137}\text{Cs}$  per unit of dry matter (DM) ( $\text{Bq}\cdot\text{kg}^{-1}$  DM). All measured activities were corrected for radioactive decay to each sampling date.

In this paper, the average values of soil properties and r-Cs content in 0–2.5 cm from the three positions (top, middle, and bottom) were calculated and are presented for each plot (Table 2). It related in terms that the 90% of r-Cs at the studied plots is accumulated in surface soil (Fig. 2), and only this layer is involved in erosion processes; therefore, this research focuses on r-Cs concentration in sediments and runoff. Figure 2 also demonstrated that mostly, the highest concentration of r-Cs is found in the middle and lower parts of the slopes that indicate downslope radionuclide migration due to soil erosion and also related with initial redistribution after Fukushima NPP accident (Komissarov and Ogura 2017).

The runoff and soil loss from the investigated slopes were monitored using 4-m-long sediment traps (weirs), which were installed in each plot in October 2013. The construction was carried out based on Robichaud and Brown (2002) and Konz et al. (2012). The plots were chosen based on their topography; each plot had clearly defined side boundaries in that the slopes were neither concave nor convex. The surface runoff and turbidity measurements, and the water sampling for r-Cs

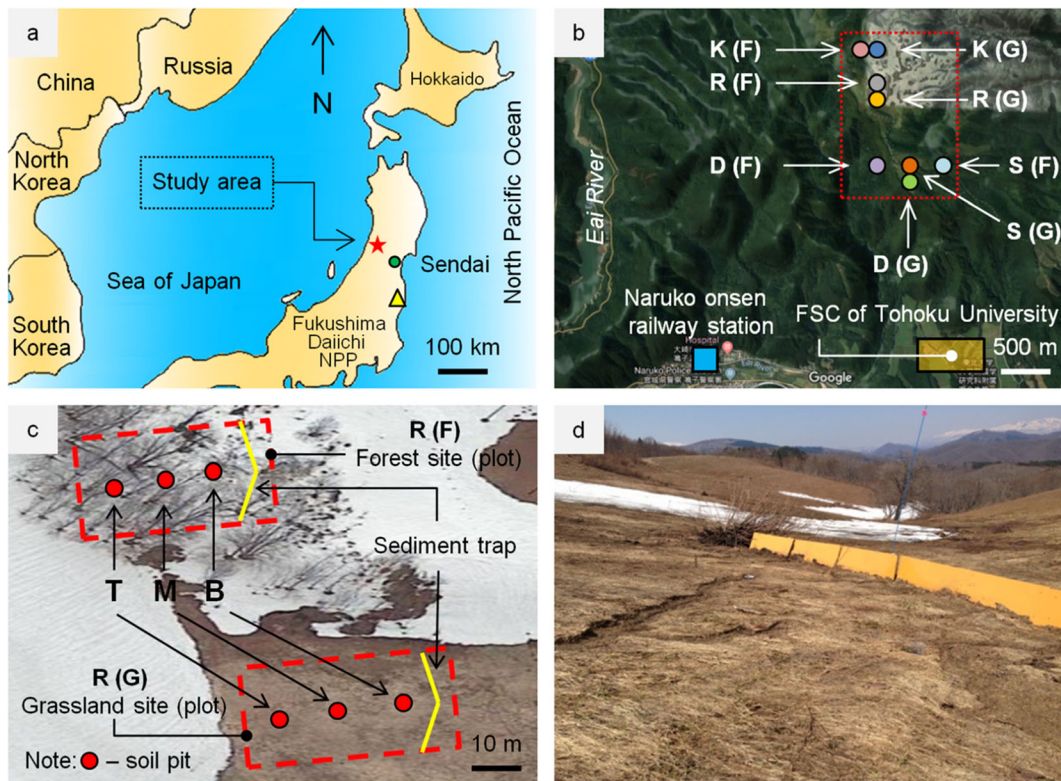


**Fig. 1** **a** General view and positions of the research area, and the Fukushima Daiichi NPP. **b** Locations of the Field Science Centre (FSC) of Tohoku University and the studied catchments: Daishaku (D), Susuki (S), Rokaku (R), and Katsurashimizu (K); G

grassland, F forest. **c** Schematics from research arrangements in Rokaku catchment and sitting of soil pits: T top, M middle, B bottom part of slope. **d** A sediment trap on Rokaku grassland plot

concentration determination, were taken every 3 h from 9:00 a.m. to midnight from the experimental weirs. No observations were performed at night, because the air temperature was predominantly negative, and runoff was absent at this time. The water turbidity measurements were taken in situ with a portable water quality meter (WOC 24, Springfield, NJ, USA). Soil loss was assessed by measuring the content of suspended sediments using a turbidity meter (Surmach 1976) and sediment tank, which were installed at the outlet of the sediment trap. The sediment tank included a geotextile which acted as a filter to separate the solids from the water. Soil conglomerates and particles were fixed by the geotextile and removed and weighed after the snow-melt period (April–May).

Measurements of the depth and density of the snow cover were taken in the grassland and forest plots during the period of stable snow cover (December–May), and route surveys were carried out every month. The depth of the snow cover was determined with a portable snow stake in the top, middle, and bottom parts of the slopes.

The snow density was measured with a snow density gauge. The soil freezing depth and soil temperature were measured using a digital soil thermometer (Custom CT-1200 D, Tokyo, Japan). The water permeability of the soil was determined by the cylinder method (Johnson 1963) using infiltrometer rings (Fig. 6). Air dose rate was determined using the Aloka  $\gamma$  survey meter (TCS-172B, Hitachi Aloka Medical, Tokyo, Japan) 1 m above the ground (snow cover). The Aloka  $\gamma$  survey meter continuously displays the air dose rate. The meter was turned on in the field, and once the display had stabilized (usually after about 30 s), three measurements were recorded over 1 min. The average of the three measurements was calculated. Before each field survey, the  $\gamma$  meter was verified by specialists in accordance with the technical regulation, and the device was calibrated using a standard gamma-ray source.

To minimize systematic errors, all field measurements (snowpack depth, soil temperature, water permeability, air dose rate measurements, soil sampling) and laboratory analyses (soil bulk density, particle size

**Table 1** Characterization of the experimental catchments

Name of catchment	Type of plot	Angle, °	Aspect relatively of slope direction, °	Geographical positions and altitude, m a.s.l.	Length of slope, m	Vegetation cover, % (top, middle, bottom)	Dominant plant species (top, middle, bottom)	Dominant tree species, height (m) and density on 10 m <sup>2</sup>
Daishaku	G	12	SE, 139	N 38° 46' 09.3" E 140° 44' 49.1" 593	111	89	<i>Rumex acetosella</i>	<i>Quercus serrata</i> , 8–12, 9
						93	<i>Rumex acetosella</i> , <i>Anthoxanthum odoratum</i>	
						94	<i>Rumex acetosella</i>	
Susuki	F	11	SW, 230	38° 46' 08.2" 140° 44' 47.9" 582	31	44	<i>Ilex dentata</i> , <i>Carpinus laxiflora</i>	
						34	<i>Carpinus laxiflora</i>	
						11	<i>Pleioblastus chino</i>	
Susuki	G	20	SE, 134	38° 46' 13.9" 140° 44' 53.3" 584	31	87	<i>Miscanthus sinensis</i> , <i>Sasa palmata</i>	
						93	<i>Miscanthus sinensis</i>	
						96	<i>Miscanthus sinensis</i>	
Rokaku	F	15	SW, 215	38° 46' 13.6" 140° 44' 57.5" 590	20	23	<i>Rubus palmatus</i>	<i>Hydrangea paniculata</i> , <i>Carpinus laxiflora</i> , 5–12, 15
						37	<i>Viola verecunda</i> , <i>Carex lanceolata</i>	
						44	<i>Carex lanceolata</i>	
Katsurashimizu	G	11	E, 71	38° 46' 37.9" 140° 44' 32.3" 607	47	97	<i>Agrostis gigantea</i>	<i>Acer rufinerve</i> , <i>Alnus hirsuta</i> , 3–7, 21
						98	<i>Rumex acetosella</i>	
						99	<i>Carex albata</i>	
Katsurashimizu	F	22	E, 74	38° 46' 41.5" 140° 44' 29.7" 616	38	30	<i>Rhododendron kaempferi</i>	
						34	<i>Weigela hortensis</i>	
						44	<i>Hydrangea serrata</i> , <i>Weigela hortensis</i>	
Katsurashimizu	G	11	NW, 324	38° 47' 04.4" 140° 44' 09.3" 610	46	92	<i>Anthoxanthum odoratum</i>	<i>Quercus crispula</i> , <i>Acer rufinerve</i> , 10–15, 7
						95	<i>Anthoxanthum odoratum</i>	
						98	<i>Anthoxanthum odoratum</i> , <i>Carex albata</i>	
Katsurashimizu	F	13	N, 25	38° 47' 04.2" 140° 44' 08.1" 618	38	19	<i>Metanarthecium luteoviride</i>	
						18	<i>Fraxinus lanuginosa</i>	
						7	<i>Rhododendron kaempferi</i>	

G grassland, F forest

**Table 2** Physicochemical properties and radiocesium concentration in soil and snowmelt sediments

Sampling site		Particle size distribution, %			Bulk density (g·cm <sup>-3</sup> )	Organic matter, %	Cesium, Bq·kg <sup>-1</sup>	
		Sand	Silt	Clay			<sup>134</sup> Cs	<sup>137</sup> Cs
Average in slope (0–2.5 cm)	Daishaku, G	50.5 ± 2.4	48.5 ± 2.3	1.0 ± 0.05	0.67 ± 0.03	6.9 ± 0.3	324 ± 12	1041 ± 31
	Daishaku, F	57.4 ± 2.7	42.2 ± 2.1	0.4 ± 0.01	0.60 ± 0.03	5.3 ± 0.1	512 ± 20	1484 ± 38
	Susuki, G	66.7 ± 2.9	31.7 ± 1.2	1.5 ± 0.04	0.57 ± 0.03	6.3 ± 0.2	979 ± 35	2815 ± 71
	Susuki, F	61.3 ± 2.1	37.6 ± 1.1	1.1 ± 0.05	0.56 ± 0.02	6.7 ± 0.2	825 ± 27	2417 ± 59
	Rokaku, G	51.0 ± 2.4	47.4 ± 2.1	1.6 ± 0.06	0.74 ± 0.04	7.0 ± 0.3	155 ± 7	489 ± 21
	Rokaku, F	50.0 ± 2.0	49.2 ± 2.0	0.8 ± 0.02	0.63 ± 0.03	6.7 ± 0.2	274 ± 10	843 ± 42
	Katsurashimizu, G	51.6 ± 1.7	47.9 ± 2.1	0.4 ± 0.01	0.64 ± 0.03	6.8 ± 0.3	543 ± 22	1616 ± 58
	Katsurashimizu, F	63.3 ± 2.8	36.0 ± 1.7	0.6 ± 0.01	0.60 ± 0.02	7.7 ± 0.4	303 ± 14	905 ± 37
Snowmelt sediments	Daishaku, G	31.9 ± 1.0	66.4 ± 2.4	1.7 ± 0.04	0.77 ± 0.04	7.4 ± 0.3	108 ± 4	283 ± 12
	Rokaku, G	33.1 ± 1.3	65.0 ± 3.0	1.9 ± 0.09	0.65 ± 0.02	7.5 ± 0.3	95 ± 4	298 ± 11
	Katsurashimizu, G	26.5 ± 1.1	71.5 ± 2.9	2.1 ± 0.09	0.60 ± 0.01	7.9 ± 0.4	170 ± 8	552 ± 21

G grassland, F forest

distribution, organic matter, and the concentration of r-Cs in the samples) were performed in triplicate. The means ± SE present in the tables and figures were calculated using MS Excel 2007 (v. 12.0) (Microsoft Corp., Redmond, WA, USA); also, the regression analyses were made there. The significance of the differences between means was estimated by *t*-test.

## Results and discussion

The meteorological and climatic conditions in 2013 and 2014 were similar to the historical averages. In the fall of 2013, early snow fell on November 11, and stable snow cover was formed only from December 4 in all catchments. The snow cover reached the maximum depth (100 ± 6–179 ± 8 cm) by the middle of February (Fig. 3). It should be noted that permanent snow cover in winter protects the soil from freezing, which is important for snowmelt infiltration and runoff (Stähli et al. 2001; Bayard et al. 2005). The snow was thicker on the slopes with northern and eastern aspects than on the western slopes. This was most likely due to wind direction and the duration of solar radiation. Snow cover duration also depends on exposure. In the forest areas, snow first disappeared at Daishaku, then at Susuku, Rokaku, and finally at Katsurashimizu (April 10, 16, 27, and 29, respectively). The depth of the snow in the forest sites was always 15–20 cm less than in the

grasslands. The maximum depth of snow cover, and therefore the highest levels of water reserves held within the snow, was observed before snow melting. This emphasizes the increased erosion hazard for the soils on slopes in the region.

It is recognized that forest coverage affects the amount of evapotranspiration and water flow, including both flood and groundwater flow. In cold regions, forests also affect snowmelt processes (Meusburger and Alewell 2014). Mishon (2007) noted that the accumulation of snow in forests is a complex process involving many factors. The main reasons for the differences in snow reserves between the fields and forests are as follows: the amount of precipitation over the forest, which is associated with a change in the roughness of the underlying surface when air masses flow onto the forest massif; the differences in the intensity of the snow melting during the winter snow breaks; the wind-mediated transfer of snow from the fields to the forests; the differences in evaporation from the surface of the snow; and the favorable conditions for the condensation of water vapor in the forests.

The reserves of water in the snow are determined not only by the depth of the snow cover but also by the density of the snow, which varies both in time and space. In both catchments, snow density increased with air temperature, settling time, and the approaching of the snowmelt period. The minimum snow density was observed in December (0.28 ± 0.01 g cm<sup>-3</sup> in the grassland

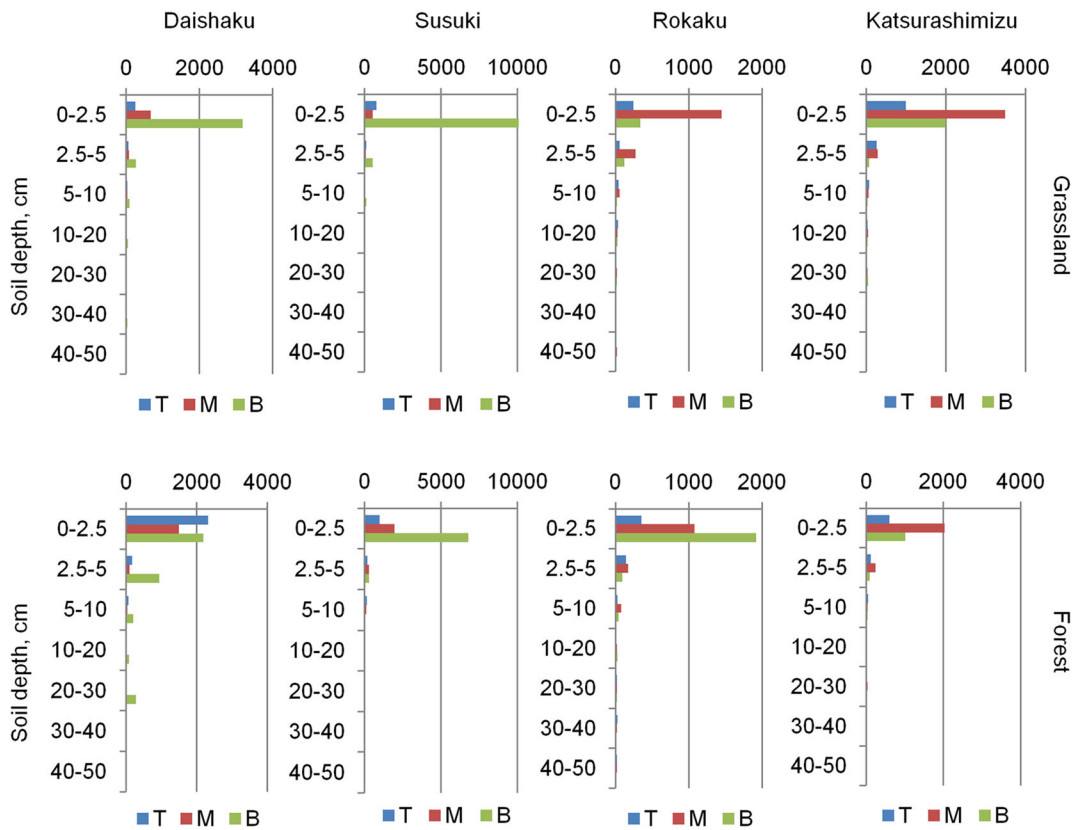


**Fig. 2** The specific activity ( $\text{Bq kg}^{-1}$ ) and distribution of total radiocesium ( $^{134}\text{Cs} + ^{137}\text{Cs}$ ) in soil profiles at studied grasslands and forested catchments; T top, M middle, B bottom part of slope

and  $0.31 \pm 0.01 \text{ g cm}^{-3}$  in the forest; the maximum density occurred in early April ( $0.48 \pm 0.01$  and  $0.52 \pm 0.01 \text{ g cm}^{-3}$ , respectively). As the depth of the snow cover increased, the density of the snow also increased; it was always higher in the forest area than in the open grassland area. In late March, snow cover became compacted, settled, temporarily melted, and partially or completely saturated with water. On all slopes, the snow density decreased from the upper to the lower parts of the watershed. In elevated areas, the snow was usually compacted by wind and snow breaks, and its depth decreased. The snow density, together with the air temperature and snow cover depth, affects soil freezing and thawing. It is known that soft snow has low thermal conductivity, which favors the protection of the soil from freezing. Conversely, compacted snow has higher thermal conductivity; therefore, compacted snow is weaker at protecting soils from cooling. The high density of snow in areas of elevated relief is one of the factors that increase the hazard of water erosion during the snowmelt period.

The soil temperature decreased from November to April and varied depending on exposition, soil properties, and protection of the soil by vegetation, i.e., the presence or absence of grass and trees in the grassland catchment and forest (Fig. 4). The lowest mean soil temperature over the observation period ( $0.1 \pm 0.003 \text{ }^\circ\text{C}$ ) was at the soil surface of the Katsurashimizu grassland. The lower temperatures in the surface soil layers in the Rokaku and Katsurashimizu were apparently related to the fact that the snow cover was established 5–10 days later and was removed 15–20 days later owing to the eastern and northern expositions. It should be noted that the soil did not freeze in any of the studied catchments. According to Niu and Yang (2006), and Ollesch et al. (2006), the soil freezing depth is one of the most important factors for the formation of surface runoff. A frozen soil layer generally increases the amount of snowmelt runoff by decreasing soil permeability and thereby impeding infiltration (Bayard et al. 2005). This results in increased soil erosion, reduced soil moisture recharge, and deep

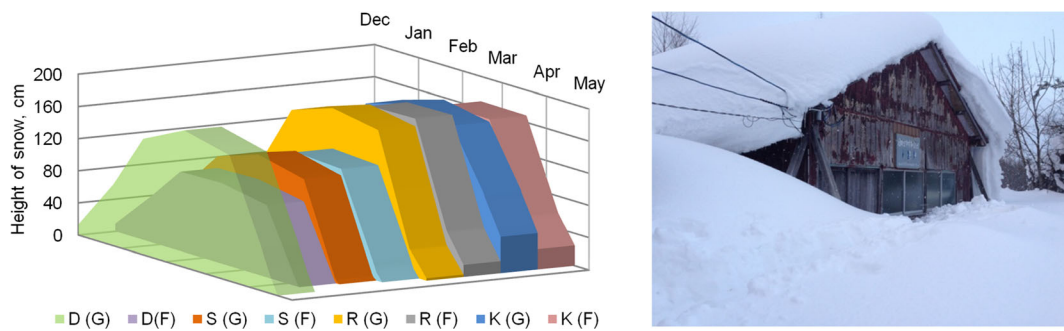


**Fig. 3** Dynamics of the snow cover depth at Daishaku (D), Susuki (S), Rokaku (R), and Katsurashimizu (K); G grassland, F Forest (left); and a photograph of a building near the Susuki catchment in the middle of January (right)

percolation (Johnsson and Lundin 1991) and an increased magnitude of the spring thaw (Unoki et al. 2003).

In Miyagi prefecture, snowmelt usually starts in mid-March and ends in early April on the plains, and lasts from mid-April to May in the mountainous areas. The duration of snowmelt depends on snow depth, meteorological conditions, the elevation of the drainage basin, and other geological features of the landscape. For example, in Hokkaido, Japan, snowmelt generally starts in mid- or late March and continues until sometime between early May and late June (Chikita 1995). The meltwater produced on the snow surface will thus infiltrate the snow mass and then discharge into a river channel as subsurface flow (Kobayashi 1985). The subsurface flow produces sediment discharge by eroding either the soil grains or the underlying bedrock debris in the porous media (Kurashige 1993).

Snow cover begins to melt when the mean daily air temperature increases past 0, and runoff usually begins at 1 °C, or 4 °C for strongly frozen soil (Komissarov and Gabbasova 2014). In any case, surface runoff begins when the rate of snowmelt exceeds the infiltration capacity of the soil. Mean daily air temperatures greater than 0 were observed by April 7, but the surface runoff began 2 days later at the Daishaku grassland, when the mean daily temperature reached  $6.1 \pm 0.1$  °C (Fig. 5). The results of our study show that the exposure of the slope and its protection by plants (grass or trees) affect the initiation and magnitude of surface flow and the initiation of snow removal from slopes. Surface runoff was only recorded in the grassland areas, where it initially began on the slopes with a southern aspect, then on those with a western aspect, and finally on those with a northern aspect. In the forests, the runoff was not recorded because most of the melt water sunk into the soil

under the snow owing to the particularly high permeability of the soil (Fig. 6). This was due to the litter layer, roots, and the looser soil texture (the soil bulk density in the 0–20-cm layer varied from  $0.67 \pm 0.02$  to  $0.74 \pm 0.02$  g cm<sup>-3</sup>). This was delayed in the field slopes with grassland, indicating that the soil texture was important. Its values varied in the profile from  $0.78 \pm 0.02$  to  $0.91 \pm 0.02$  g cm<sup>-3</sup>. The litter layer is also a factor that reduces overland flow by inhibiting crust formation in forests (e.g., Banzai 1997; Bissonnais et al. 1998). Plant root development can improve soil physical properties (e.g., soil strength, shear strength, structural stability, and aggregate stability), which are closely related to soil erodibility and can therefore limit soil losses through erosion (Komissarov and Gabbasova 2017). The volume of surface runoff in the grassland catchments was temporally variable and was dependent on air temperature and exposition. The most intensive runoff was usually observed in the days with high air temperatures. The runoff ended when the snow was completely removed from the slopes by April 21, 22 and 30 for Daishaku, Rokaku, and Katsurashimizu, respectively (Fig. 5). Surface runoff was not observed at the Susuki grassland; it was transformed to subsurface runoff because the soil did not freeze, had a good texture, and high water permeability (Fig. 6); a potuscular transition to groundwater also took place. According to data pertaining to water permeability and runoff (Fig. 5), surface runoff forms in the Miyagi mountain area when the infiltration speed of snowmelt water into the soil remains below 0.13 mm min<sup>-1</sup> for 7 h. When the infiltration speed was higher than this value, no runoff was observed.

The maximum water reserves in the snow before the snowmelt in the grasslands at Daishaku, Rokaku, and Katsurashimizu were almost similar:  $75 \pm 2$ ,  $82 \pm 2$ , and



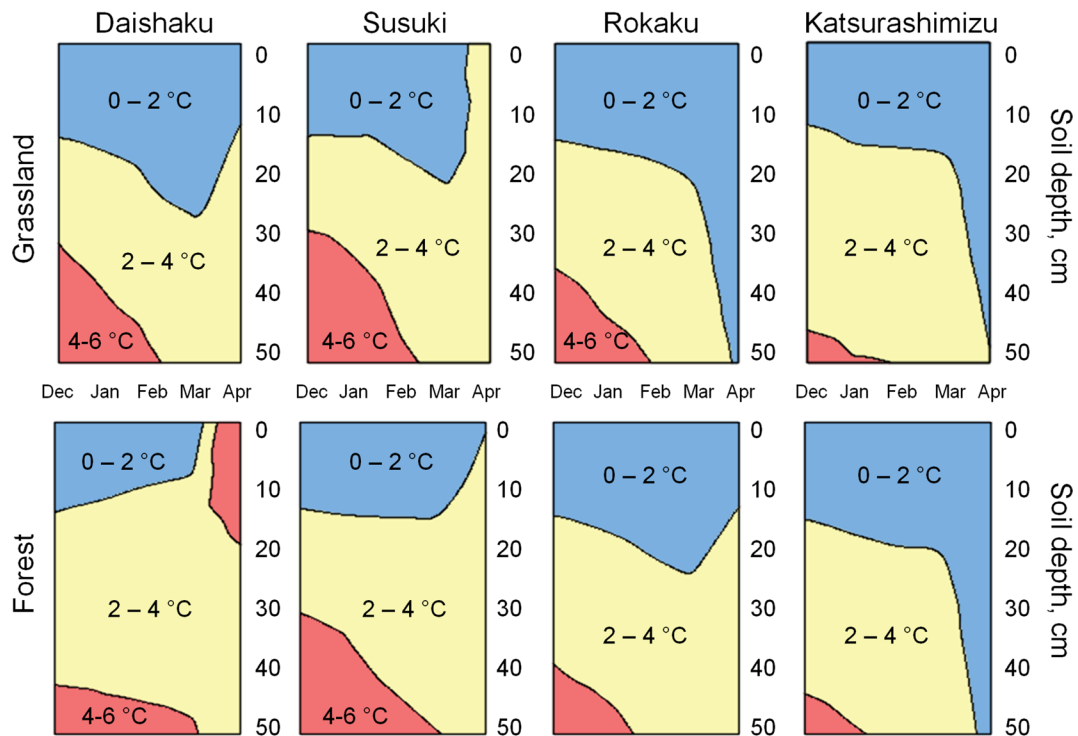


**Fig. 4** Temperature of the soils in the different catchments from December 2013 to April 2014

73 ± 2 mm, respectively; the total volume of the surface runoff in the same catchments was 37 ± 2, 31 ± 2, and 52 ± 2 mm, respectively (Fig. 5). Thus, approximately 50% (runoff coefficient 0.49 ± 0.02, 0.38 ± 0.02, and 0.71 ± 0.02) of the surface melt water from grassland slopes could fall through the hydrographic system to the final links of the erosion channel system (rivers, lakes, and ponds) and remove solid phase soil and many soluble chemical elements and pollutants. The spring water is insufficient for the replenishment of the soil reserves. At the same time, the forest litter layer remaining on the surface of the soil retains the solid runoff and preserves the accumulated water, which largely facilitates the functioning of terrestrial geosystems. It is interesting to note that in 2014, for the summer-fall period at Daishaku site, the total surface liquid runoff was 237 mm or six times higher than that in snowmelt. But the runoff coefficient for the warm season (0.22) was two times lower than that in spring. Such differences are related with terms of soil conditions, e.g., water permeability. The infiltration capacity of soil during the snowmelt period was therefore lower ( $p < 0.01$ ) than in summer as the soil was already saturated with water at the start of winter (Komissarov and Ogura 2020). Furthermore, the vegetation cover, root network, and sward

were weakly developed in spring, contributing to increased flow.

The highest runoff rate (42 ± 1 L s<sup>-1</sup> ha<sup>-1</sup>) was observed in the Katsurashimizu grassland at 1:00 p.m. on April 27 when the air temperature reached 21.8 ± 0.4 °C. Suspended sediment contents in this case constituted 4.1 ± 0.1 mg L<sup>-1</sup>. The highest water flow turbidity, 6.1 ± 0.2–10.5 ± 0.2 NTU (3.5 ± 0.1–6.1 ± 0.1 mg·L<sup>-1</sup>), was recorded in the Daishaku grassland on April 16–17. The content of suspended sediments in all catchments was insignificant in the first days of the snowmelt but abruptly increased by the end of the snowmelt period after the appearance of thaw patches. It varied proportionally to the runoff rate, i.e., most of the fertile soils were removed in the last days of the snowmelt. This is due to the fact that the nearly or disappeared (melted) snow no longer filters suspended sediments, and when the runoff is formed on the soil surface, the micro-rills appear, then the snowmelt flow easily detached/transported the soil particles. Similar results were obtained in the other climatic conditions (Ollesch et al. 2006; Tanasienko et al. 2009; Meusburger and Alewell 2014; Komissarov and Gabbasova 2014). It should be noted that soil erosion decreased with increasing content of suspended sediments in the water flow. The reason

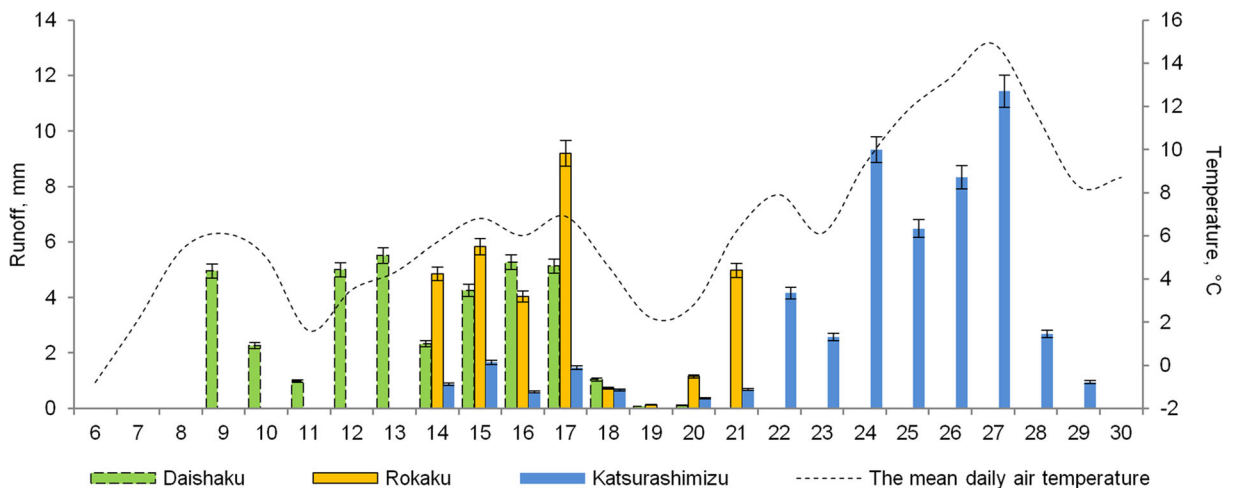


**Fig. 5** The runoff and mean daily air temperature during the active snowmelt period (from April 6 to 30)

for this is related to the silting of the interaggregate pores with sediments increasing adhesion between the aggregates (Larionov et al. 2008).

On December 22, 2011 the Japanese government announced new limits for radioactive cesium in foods and drinking water, which have been enforced since April 2012 (MHLW 2011). The new standard limits for radioactive cesium are established so that effective doses of radionuclides (including Sr-90, Ru-106, and Pu) do not exceed  $1 \text{ mSv year}^{-1}$ . According to these new standards, the maximum concentration of cesium (the sum of  $^{134}\text{Cs}$  and  $^{137}\text{Cs}$ ) allowed in drinking water is  $10 \text{ Bq kg}^{-1} (\text{L}^{-1})$  ( $100 \text{ Bq kg}^{-1}$  in food vegetation). By comparison, the US Environmental Protection Agency (EPA) sets a maximum of  $3700 \text{ Bq m}^{-3}$  ( $3.7 \text{ Bq kg}^{-1} (\text{L}^{-1})$ ) in drinking water (international standards).

Whereas the surface soil is highly polluted by r-Cs (Table 2), the total Cs (total Cs =  $^{134}\text{Cs}$  +  $^{137}\text{Cs}$ ) concentration in runoff samples, which were taken throughout

the flow depth every day during the snowmelt period from all catchments, did not exceed  $10 \text{ Bq L}^{-1}$  (varying from  $0.1 \pm 0.1$ – $8.4 \pm 0.1 \text{ Bq L}^{-1}$ ) and can therefore be considered ecologically safe. This is consistent with the findings from a previous study that after an initial runoff following deposition, less than 0.1% of the  $^{137}\text{Cs}$  dissolves into solution per year (Ritchie 1998). In a laboratory study, Dagleish and Foster (1996) showed that  $^{137}\text{Cs}$  can be adsorbed by particles already entrained in the runoff. Up to 10% of applied  $^{137}\text{Cs}$  was lost from compacted soil in eroded sediments, whereas a maximum of 2.03% was contained in solution in the runoff. It should be noted that in the snow, which was sampled every month, the total Cs concentration was also low ( $0.7 \pm 0.1$ – $7.4 \pm 0.1 \text{ Bq L}^{-1}$ ). And in the summer-fall period for Daishaku site, it also did not exceed  $10 \text{ Bq L}^{-1}$ , even in extreme events with high intensity of rainfall: in October 2014, about 200 mm of rainfall was recorded over almost 2 weeks with highest runoff

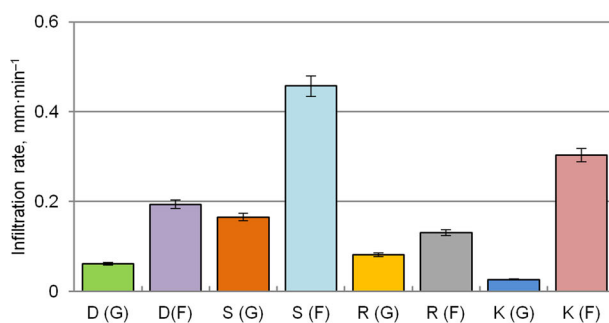


**Fig. 6** Water permeability (average over 7 h) of the soil during the active snowmelt period (April 11, 2014 at Daishaku (D) and Susuki (S); April 18 at Rokaku (R), and April 22 at



Katsurashimizu (K); G grassland, F forest) (left); and measuring process by cylinder (right)

(70 mm) (Komissarov and Ogura 2020). This may be because r-Cs is adsorbed onto soil particles, and, in this case, surface runoff can be partially delayed by sods.

The surface soil at the sampling site is a silty sandy loam (Table 2) according to the Unified Soil Classification System of Japan, and the sediments were classified as organic silt. The organic matter in the surface soil had a high humus content. Soil with higher silt and organic matter content can have increased soil infiltration and soil aggregates, resulting in good structural stability and leading to reduced runoff and erosion (Komissarov and Gabbasova 2017). Humus is responsible for soil structure formation and stability against erosion and accounts for the low proportion of solid compounds in the runoff (Elliott 1986). Humus is known to stabilize aggregates, as organic functional groups bind to highly reactive sesquioxides and clays and contribute to soil structure formation (Bogdanov 1964).

Following deposition on the soil surface, r-Cs is strongly fixed by colloidal clay fraction and organic particles (He and Walling 1996; Ritchie 1998). The absorption intensity of r-Cs to soil is dependent on a number of factors, including clay structure (presence of illite and vermiculite), concentrations of Cs and competing ions such as  $K^+$ ,  $Ca^{2+}$ ,  $Mg^{2+}$ , and  $NH_4$  and solution pH (Fuller et al. 2015). The concentration of r-Cs in the sediments was lower compared to the slope surface soil (Table 2) but higher than permissible level values ( $100 \text{ Bq kg}^{-1}$ ); thus, a potential contamination of grass on pastures occurred, which depends from many factors (meteorological conditions, soil properties, root uptake, weathering etc. (Burger and Lichtscheidl 2018) and required the extra research on studied sites. Saturation of sediments by r-Cs is due to the fact that, while moving along the surface of slopes, snowmelt runoff leaches fine Cs-rich particles from the soil. During the erosion phase, the fine and Cs-rich particles are more easily transported, while a larger proportion of coarse particles, with low r-Cs content, will settle when the carrying capacity of the runoff is reduced or exceeded (He and Walling 1996).

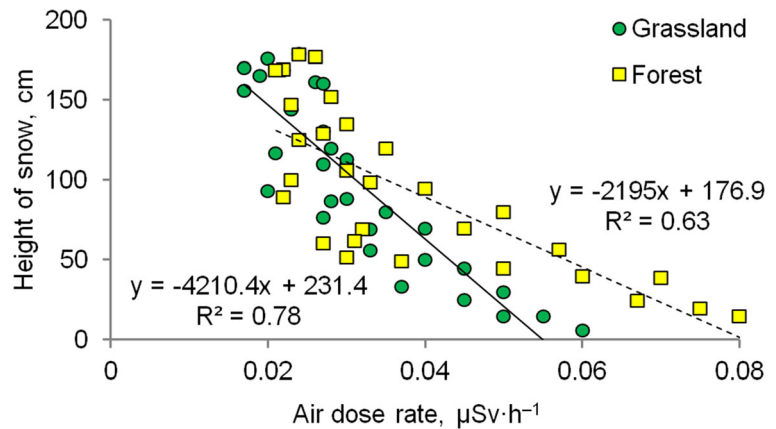
The trapped sediments had a slightly higher organic matter content than the surface soil, on average 0.4% higher (Table 2). The surface runoff was accompanied by the selective removal of small, fine soil particles (silt and clay), which have high organic matter content (Komissarov and Klik 2020). Small-sized soil particles contain more organic matter than larger aggregates (Rumpel et al. 2006). It should be noted that drift soils

rich in humus and nutrients are formed at the deposition of sediments in the lower parts of the slopes. Their humus reserves are often several times larger than those in the non-eroded soil. However, Gabbasova et al. (2016) considered that the excessive depth and humus content of drift soils cannot be completely utilized by plants and forms a sort of dead preserved humus reserve.

The highest soil losses during the snowmelt period were observed on the southern slope in the Daishaku grassland (according to calculated turbidity measurements and sediment weights from the accumulation tank) and consisted of approximately  $6\text{--}9 \text{ kg ha}^{-1}$ . From Rokaku (eastern slope) and Katsurashimizu (northern slope) grasslands, losses were approximately 2–4 and  $6\text{--}7 \text{ kg ha}^{-1}$ , respectively, indicating that the amount of removed material primarily depended on exposure. It should be noted that the rate of soil formation on a global scale is  $370\text{--}1290 \text{ kg ha}^{-1} \text{ year}^{-1}$  (mean = 700) (Wakatsuki and Rasyidin 1992); thus, snowmelt erosion rates on grassland slopes can be considered as harmless (excluding deflation and rainfall erosion). Even with adding the soil loss caused by rainfalls from Daishaku pasture catchment slope, which amounted to  $23 \text{ kg ha}^{-1}$  (Komissarov and Ogura 2020), the total erosion rates ( $\sim 32 \text{ kg ha}^{-1} \text{ year}^{-1}$ ) are characterized as low. On the other grassland slope expositions, the soil losses caused by rainfalls were  $\sim 9$  (Rokaku) and  $\sim 18 \text{ kg ha}^{-1}$  (Katsurashimizu), with total erosion  $\sim 12$  and  $24 \text{ kg ha}^{-1} \text{ year}^{-1}$ , respectively. Under forest sites and grassland covered by *Miscanthus sinensis* (Japanese silver grass) there is no soil erosion were observed. Thus, for the dominant grasslands (in the study area), the snowmelt soil loss is about 3 times lower than that caused by rainfalls. For example, in the Cis-Ural region of Russia, the soil loss caused by snowmelt on grasslands with gentle slopes averages  $20 \text{ kg ha}^{-1} \text{ year}^{-1}$  (Komissarov and Gabbasova 2014). The sediments from the Katsurashimizu grassland contained higher levels of r-Cs, clay, and organic matter because the rate of the runoff was low. In the Daishaku and Rokaku catchments, when runoff rates were high, the snowmelt also leached sand particles with low levels of r-Cs and organic matter.

For the Miyagi prefecture, the average, maximum, and minimum dose rates were estimated to be 0.15, 0.25, and  $0.10 \mu\text{Sv h}^{-1}$ , respectively (Satho 1987). In the Oshika Peninsula and neighboring areas that comprise Paleozoic-Mesozoic sedimentary rocks, the dose rate is relatively higher than in other parts of the

**Fig. 7** Relationship between the air dose rate and the depth of snow ( $p < 0.001$ ,  $n = 122$ ); solid and dashed—linear trends for grasslands and forests sites, respectively



prefecture (Furukawa and Shingaki 2012). Bruno (2011) measured the air dose rate (1 m above ground level) from May 24 to June 3, 2011. Approximately 60 km north of the Fukushima Daiichi NPP, the air dose rate in Marumori (Miyagi prefecture) was found to be  $0.47 \mu\text{Sv h}^{-1}$ .

Our measurements suggest that the air dose rate was always lower than the maximum permissible concentration ( $0.2 \mu\text{Sv h}^{-1}$ ) and varied from  $0.02 \pm 0.001$  to  $0.09 \pm 0.003 \mu\text{Sv h}^{-1}$  in winter and from  $0.08 \pm 0.002$  to  $0.13 \pm 0.004 \mu\text{Sv h}^{-1}$  at the times of the year without snow (May–October 2014). During periods of stable snow cover, the air dose rate increased with decreasing snow thickness (Fig. 7). This is due in the changing of the measurement distance from the soil surface and the Aloka  $\gamma$  survey meter (due to changes in snow height), and on the other hand, snow absorbs radioactive emissions and acts as a protective screen, as previously suggested by Komissarov and Ogura (2017). In the forest catchments, the air dose rate was always slightly higher compared with those from open areas in all seasons. This is probably due to the understanding that coniferous forests are known to be very efficient filters of airborne  $^{131}\text{I}$  and r-Cs under conditions of dry deposition (e.g., Bunzl et al. 1989; Livens et al. 1992). Bunzl et al. (1989) observed 20% higher r-Cs deposition in a spruce forest compared with a nearby grassland.

## Conclusions

The period of spring snowmelt can be subdivided into two stages depending on the snow cover area

in the catchment and the presence of thaw patches. The first stage of the snowmelt period in all catchments, i.e., when the runoff of melt water passed, was filtered through the snow layer, flowed on the surface of the non-frozen soil with sandy loam texture, and was characterized by similar concentrations of suspended sediments. During the second stage, the surface runoff began to detach soil particles from the thawed surface areas when melt water flowed over the wet surface; the content of the suspended sediments significantly increased with higher runoff volumes and rates. Thus, the greatest soil losses are observed in the last days of snowmelt; this phenomenon is obvious and in correspondence with other studies. In the final stage of snowmelt, the removal of particles of 2–50  $\mu\text{m}$  was most dominant. The suspended sediment consisted of up to 68–73% of fine particles, represented mostly by silt. The r-Cs concentration in sediments was up to 60% of the r-Cs concentration in soils on adjoining slopes; thus, there is considerable lateral r-Cs migration during snowmelt. However, the r-Cs concentration in runoff samples was below the permissible level ( $10 \text{ Bq L}^{-1}$ ).

Soil loss in grasslands induced by snowmelt runoff is low ( $2\text{--}9 \text{ kg ha}^{-1}$ ) and depends on slope exposition. There was no surface runoff (snowmelt erosion) in forested areas and grasslands covered by *Miscanthus sinensis* (Japanese silver grass). The leaf litter layer and vegetation protect the soil surfaces, increase soil surface roughness, impede overland flow, and increase infiltration. Preliminarily, we can conclude that the spring snowmelt accounted for about 15% of liquid runoff and 30% of sediment runoff at grasslands on the mountain slopes of Miyagi Prefecture.

**Acknowledgments** The authors are grateful to the “Japan-Russia Youth Exchange Center” Foundation that provided us with the opportunity to conduct this research. Special thanks to Prof. Y. Onda and H. Kato from the University of Tsukuba for allowing us to use their laser diffraction particle size analyzer.

**Funding information** This study was funded by the “Japan-Russia Youth Exchange Center” Foundation through the JREX Fellowship program.

**Compliance with ethical standards**

**Conflict of interest** The authors declare that they have no conflict of interest.

**References**

Ashida, K., & Kira, H. (1975). Aspects of environmental changes. In T. Ishiwhara (Ed.), *Studies on environmental changes due to sediment yield and transport*. Cooperative Research Group of Natural Disasters. Report No. A-50-9, Kyoto, pp. 7–31. (In Japanese).

Banzai, K. (1997). Study on crust formation and its effect on rainwater infiltration and soil erosion of bare slopes. *Bulletin of National Institute for Agro-Environmental Sciences*, 14, 49–95 (In Japanese with English summary).

Bayard, D., Stahl, M., Parriaux, A., & Fluhler, H. (2005). The influence of seasonally frozen soil on the snowmelt runoff at two Alpine sites in southern Switzerland. *Journal of Hydrology*, 309, 66–84. <https://doi.org/10.1016/j.jhydrol.2004.11.012>.

Bissonnais, L., Benkhadra, Y. H., Chaplot, V., Fox, D., King, D., & Daroussin, J. (1998). Crusting, runoff and sheet erosion on silty loamy soils at various scales and upscaling from m<sup>2</sup> to small catchments. *Soil and Tillage Research*, 46, 69–80. [https://doi.org/10.1016/S0167-1987\(97\)00079-2](https://doi.org/10.1016/S0167-1987(97)00079-2).

Bogdanov, N. I. (1964). Humus composition in West Siberian chernozems. *Proc. Conf. of Siberia and Far East Soil Scientists*, SB. AS. USSR, Novosibirsk, 312–322. (In Russian).

Bruno, C. (2011). Consequences of the Fukushima Daiichi accident in Japan: a substantial and long-lasting contamination *CRIRAD*, July 7, 2011 Communiqué.

Bunzl, K., Schimmack, W., Kreutzer, K., & Schierl, R. (1989). Interception and retention of Chernobyl-derived <sup>134</sup>Cs, <sup>137</sup>Cs and <sup>106</sup>Ru in a spruce stand. *Science of the Total Environment*, 78, 77–87. [https://doi.org/10.1016/0048-9697\(89\)90023-5](https://doi.org/10.1016/0048-9697(89)90023-5).

Burger, A., & Lichtscheidl, I. (2018). Stable and radioactive cesium: a review about distribution in the environment, uptake and translocation in plants, plant reactions and plants’ potential for bioremediation. *Science of the Total Environment*, 618, 1459–1485. <https://doi.org/10.1016/j.scitotenv.2017.09.298>.

Chikita, K. A. (1995). Suspended sediment discharge from snowmelt: Ikushunbetsu River, Hokkaido, Japan. *Journal of Hydrology*, 186, 295–313. [https://doi.org/10.1016/S0022-1694\(96\)03021-1](https://doi.org/10.1016/S0022-1694(96)03021-1).

Classification Committee of Cultivated Soils, (1996). Soil classification for cultivated soils in Japan 3rd approximation. *Miscellaneous Publication of the National Institute of Agro-Environmental Sciences*, 17, Tsukuba.

Dalglish, H. Y., & Foster, I. D. L. (1996). <sup>137</sup>Cs losses from a loamy surface water gleyed soil (Inceptisol): a laboratory simulation experiment. *Catena*, 26, 227–245. [https://doi.org/10.1016/0341-8162\(96\)00002-1](https://doi.org/10.1016/0341-8162(96)00002-1).

Demidov, V. V., Ostroumov, V. Y., Nikitishena, I. A., & Lichko, V. I. (1995). Seasonal freezing and soil erosion during snowmelt. *Eurasian Soil Science*, 28, 78–87.

Dube, A., & Mailloux, A. (1969). La mesure de l’érosion à Cap-aux-Corbeaux. *Agriculture*, 26, 32–36.

Elliott, E. T. (1986). Aggregate structure and carbon, nitrogen, and phosphorus in native and cultivated soils. *Soil Science Society of America Journal*, 50, 627–633. <https://doi.org/10.2136/sssaj1986.03615995005000030017x>.

Fuller, A. J., Shaw, S., Ward, B. M., Haigh, S. J., Mosselmans, J. F. W., Peacock, C. L., Stackhouse, S., Dent, A. J., Trivedi, D., & Burke, I. T. (2015). Caesium incorporation and retention in illite interlayers. *Applied Clay Science*, 108, 128–134. <https://doi.org/10.1016/j.clay.2015.02.008>.

Furukawa, M., & Shingaki, R. (2012). Terrestrial gamma radiation dose rate in Japan estimated before the 2011 great east Japan earthquake. *Radiation Emergency Medicine*, 1, 11–16.

Gabbasova, I. M., Suleimanov, R. R., Khabirov, I. K., Komissarov, M. A., Fruehauf, M., Liebelt, P., Garipov, T. T., Sidorova, L. V., & Khaziev, F. K. (2016). Temporal changes of eroded soils depending on their agricultural use in the southern Cis-Ural region. *Eurasian Soil Science*, 49, 1204–1210. <https://doi.org/10.1134/S1064229316100070>.

Grismer, M. E. (2013). Stream sediment and nutrient loads in the Tahoe Basin – estimated vs monitored loads for TMDL “crediting”. *Environmental Monitoring and Assessment*, 185, 7883–7894. <https://doi.org/10.1007/s10661-013-3142-2>.

He, Q., & Walling, D. E. (1996). Interpreting particle size effects in adsorption of <sup>137</sup>Cs and unsupported <sup>210</sup>Pb by mineral soils and sediments. *Journal of Environmental Radioactivity*, 30, 117–137. [https://doi.org/10.1016/0265-931X\(96\)89275-7](https://doi.org/10.1016/0265-931X(96)89275-7).

International Atomic Energy Agency (2011). Impact of soil conservation measures on erosion control and soil quality. *IAEA-TECDOC-1665*, Vienna.

Johnson, A. I. (1963). *A field method for measurement of infiltration*. Washington: US Government Printing Office.

Johnsson, H., & Lundin, L. C. (1991). Surface runoff and soil water percolation as affected by snow and soil frost. *Journal of Hydrology*, 122, 141–159. [https://doi.org/10.1016/0022-1694\(91\)90177-J](https://doi.org/10.1016/0022-1694(91)90177-J).

Kadomura, H. (1980). Erosion by human activities in Japan. *GeoJournal*, 4, 133–144.

Kato, H., Onda, Y., & Gomi, T. (2012). Interception of the Fukushima reactor accident-derived <sup>137</sup>Cs, <sup>134</sup>Cs and <sup>131</sup>I by coniferous forest canopies. *Geophysical Research Letters*, 39, L20403. <https://doi.org/10.1029/2012GL052928>.

- Kawagoe, S., Kazama, S., & Sarukkalinge, P. R. (2009). Assessment of snowmelt triggered landslide hazard and risk in Japan. *Cold Regions Science and Technology*, 58, 120–129. <https://doi.org/10.1016/j.coldregions.2009.05.004>.
- Kazama, S., & Sawamoto, M. (1995). Estimation of the snowdepth distribution and snowwater resources in wide area. In *In: Proceedings of the International Conference on Water Resources and Environmental Research. Towards the 21st century 1* (pp. 659–666).
- Kirby, P. C., & Mehuys, G. R. (1987). The seasonal variation of soil erosion by water in southwestern Quebec. *Canadian Journal of Soil Science*, 67, 55–63. <https://doi.org/10.4141/cjss87-005>.
- Kobayashi, D. (1985). Separation of the snowmelt hydrograph by stream temperatures. *Journal of Hydrology*, 76, 155–165. [https://doi.org/10.1016/0022-1694\(85\)90096-4](https://doi.org/10.1016/0022-1694(85)90096-4).
- Komissarov, M. A., & Gabbasova, I. M. (2014). Snowmelt – induced soil erosion on gentle slopes in the southern Cis-Ural region. *Eurasian Soil Science*, 47, 598–607. <https://doi.org/10.1134/S1064229314060039>.
- Komissarov, M. A., & Gabbasova, I. M. (2017). Erosion of agrochernozems under sprinkler irrigation and rainfall simulation in the southern forest-steppe of Bashkir Cis-Ural region. *Eurasian Soil Science*, 50, 253–261. <https://doi.org/10.1134/S1064229317020077>.
- Komissarov, M. A., & Klik, A. (2020). Impact of no-till, conservation and conventional tillage on erosion and soil properties in lower Austria. *Eurasian Soil Science*, 53, 503–511. <https://doi.org/10.1134/S1064229320040079>.
- Komissarov, M. A., & Ogura, S. (2017). Distribution and migration of radiocesium in sloping landscapes three years after the Fukushima-I nuclear accident. *Eurasian Soil Science*, 50, 861–871. <https://doi.org/10.1134/S1064229317070043>.
- Komissarov, M. A., & Ogura, S. (2020). Siltation and radiocesium pollution of small lakes in different catchment types far from the Fukushima Daiichi nuclear power plant accident site. *International Soil and Water Conservation Research*, 8, 56–65. <https://doi.org/10.1016/j.iswcr.2019.10.003>.
- Komissarov, M., Ogura, S., Kato, H., & Masanori, S. (2017). Effects of plowing on vertical distribution of radioactive Cs and soil physicochemical properties in temperate pastures. *Grassland Science*, 63, 265–272. <https://doi.org/10.1111/grs.12172>.
- Konz, N., Prasuhn, V., & Alewell, C. (2012). On the measurement of alpine soil erosion. *Catena*, 91, 63–71. <https://doi.org/10.1016/j.catena.2011.09.010>.
- Kurashige, Y. (1993). Mechanism on delayed appearance of peak suspended sediment concentration in a small river. *Trans. Japanese Geomorphological Union*, 14, 385–405.
- Lal, R. (1991). (Ed.) Sustainable development and management of land and water resources no. 1. Food and Agriculture Organization of the United Nations, Rome.
- Larionov, G. A., Dobrovolskaya, N. G., Kiryukhina, Z. P., & Litvin, L. F. (2008). Effect of suspended sediments on soil erodibility. *Eurasian Soil Science*, 41, 768–773. <https://doi.org/10.1134/S1064229308070119>.
- Lindström, G., Bishop, K., & Löfvenius, M. O. (2002). Soil frost and runoff at Svartberget, northern Sweden – measurements and model analysis. *Hydrological Processes*, 16, 3379–3392. <https://doi.org/10.1002/hyp.1106>.
- Livens, F. R., Fowler, D., & Horrill, A. D. (1992). Wet and dry deposition of  $^{131}\text{I}$ ,  $^{134}\text{Cs}$  and  $^{137}\text{Cs}$  at an upland site in northern England. *Journal of Environmental Radioactivity*, 16, 243–254. [https://doi.org/10.1016/0265-931X\(92\)90003-C](https://doi.org/10.1016/0265-931X(92)90003-C).
- Matsuura, S., Okamoto, T., Asano, S., Osawa, H., & Shibasaki, T. (2017). Influences of the snow cover on landslide displacement in winter period: a case study in a heavy snowfall area of Japan. *Environmental Earth Sciences*, 76, 362. <https://doi.org/10.1007/s12665-017-6693-7>.
- Meusburger, K., & Alewell, C. (2014). *Soil erosion in the Alps. Experience gained from case studies (2006–2013), environmental studies no. 1408*. Bern: Federal Office for the Environment.
- MHLW (2011). Submission to the Radiation Council of Japan for deliberations to set the regulation values for radioactive materials in food and water. <http://www.mhlw.go.jp/stf/houdou/2r9852000001z9vp.html>. (in Japanese).
- Mishon, V. M. (2007). *Extended abstract of doctoral dissertation in geography*. Voronezh State University (In Russian).
- Miura, S., Aoyama, M., Ito, E., Shichi, K., Takata, D., Masaya, M., Sekiya, N., Kobayashi, N., Takano, N., Kaneko, S., Tanoi, K., & Nakanishi, T. (2015). Towards prediction of redistribution of fallout radiocesium on forested area discharged from Fukushima Nuclear Power Plant. *Geophysical Research Abstracts*, 17, EGU, 8989.
- Muthanna, T. M., Viklander, M., Blecken, G., & Thorolfsson, S. T. (2007). Snowmelt pollutant removal in bioretention areas. *Water Research*, 41, 4061–4072. <https://doi.org/10.1016/j.watres.2007.05.040>.
- Niu, G. Y., & Yang, Z. L. (2006). Effects of frozen soil on snowmelt runoff and soil water storage at a continental scale. *Journal of Hydrometeorology*, 7, 937–952. <https://doi.org/10.1175/JHM538.1>.
- Ogura, S., Suzuki, T., & Saito, M. (2014). Distribution of radioactive cesium in soil and its uptake by herbaceous plants in temperate pastures with different management after the Fukushima Dai-Ichi Nuclear Power Station accident. *Soil Science and Plant Nutrition*, 60, 790–800. <https://doi.org/10.1080/00380768.2014.954269>.
- Ollesch, G., Sukhanovski, Y., Kistner, I., Rode, M., & Meissner, R. (2005). Characterization and modelling of the spatial heterogeneity of snowmelt erosion. *Earth Surface Processes and Landforms*, 30, 197–211. <https://doi.org/10.1002/esp.1175>.
- Ollesch, G., Kistner, I., Meissner, R., & Lindenschmidt, K. E. (2006). Modelling of snowmelt erosion and sediment yield in a small low-mountain catchment in Germany. *Catena*, 68, 161–176. <https://doi.org/10.1016/j.catena.2006.04.005>.
- Ritchie, J. C. (1998).  $^{137}\text{Cs}$  use in estimating soil erosion: 30 years of research. *IAEA-TECDOC*, 1028, 5–12.
- Robichaud, P. R., & Brown, R. E. (2002). *Silt fences: an economical technique for measuring hillslope soil erosion, RMRS-GTR-94, Rocky Mountain Research Station, USDA Forest Service*. Washington: United States Department of Agriculture.
- Rumpel, C., Chaplot, V., Planchon, O., Bernadou, J., Valentin, C., & Mariotti, A. (2006). Preferential erosion of black carbon on steep slopes with slash and burn agriculture. *Catena*, 65, 30–40. <https://doi.org/10.1016/j.catena.2005.09.005>.

- Satho, K. (1987). Gamma radiation dose rate in air in Miyagi prefecture. *Annual report of Environmental Radioactivity Research Institute of Miyagi*, 6, 13–16.
- Sayer, C. D., & Neil, R. (2001). Establishing realistic restoration targets for nutrient enriched shallow lakes: linking diatom ecology and palaeoecology at the Attenborough ponds, U.K. *Hydrobiologia*, 448, 117–142. <https://doi.org/10.1023/A:1017597221052>.
- Soil Survey Staff. (1999). *Soil taxonomy: a basic system of soil classification for making and interpreting soil surveys, 2nd ed*, US Department of Agriculture Handbook 436. Washington: Natural Resources Conservation Service.
- Stähli, M., Nyberg, L., Mellander, P. E., Jansson, P. E., & Bishop, K. H. (2001). Soil frost effects on soil water and runoff dynamics along a boreal transect: 2. Simulations. *Hydrological Processes*, 15, 927–941. <https://doi.org/10.1002/hyp.232>.
- Summach, G. P. (1976). *Water erosion and its control*. Leningrad: Gidrometeoizdat (In Russian).
- Tanasienko, A. A., Yakutina, O. P., & Chumbaev, A. S. (2009). Snowmelt runoff parameters and geochemical migration of elements in the dissected forest-steppe of West Siberia. *Catena*, 78, 122–128. <https://doi.org/10.1016/j.catena.2009.03.008>.
- Unoki, K., Yamamoto, T., Inoue, T., Nagasawa, T., & Okazawa, H. (2003). River water quality and hydrological condition of dairy farming watershed during snowmelt and ground thawing period. *Trans. Japanese Society of Irrigation, Drainage and Reclamation Engineering*, 228, 9–15. (In Japanese with English abstract).
- Uri, N. D. (2001). Agriculture and the environment – the problem of soil erosion. *Journal of Sustainable Agriculture*, 16, 71–91. [https://doi.org/10.1300/J064v16n04\\_07](https://doi.org/10.1300/J064v16n04_07).
- Wakatsuki, T., & Rasyidin, A. (1992). Rates of weathering and soil formation. *Geoderma*, 52, 251–263. [https://doi.org/10.1016/0016-7061\(92\)90040-E](https://doi.org/10.1016/0016-7061(92)90040-E).
- Yoshihara, Y., & Sato, S. (2013). Seasonal change and distribution of grass nutritive values and minerals in an open pasture surrounded by forest. *Agroforestry Systems*, 87, 901–907. <https://doi.org/10.1007/s10457-013-9606-0>.
- Yoshikawa, T. (1974). Denudation and tectonic movement in contemporary Japan. *Bulletin of the Department of Geography, University of Tokyo*, 6, 1–14.

**Publisher's note** Springer Nature remains neutral with regard to jurisdictional claims in published maps and institutional affiliations.